

Source Rock Evaluation of Shemshak Formation in the Central Alborz Basin: A Preliminary Investigation

Rahimpour-Bonab¹, H., Zamani², Z. and M.R. Kamali²

1-Department of Geology, Faculty of Science, University of Tehran,

P. Box 14155-6455, Tehran, Iran,

Email: rahimpour@khayam.ut.ac.ir

2- Research Institute, National Iranian Oil Company, Tehran, Iran

(received: 7/9/2001 ; accepted: 9/30/2002)

Abstract

This paper outlines the organic petrology and geochemistry of potential hydrocarbon source rocks from southern Caspian Basin. Coals and associated beds from Kalaris member of the Shemshak Formation in the southern Caspian Basin were analyzed megascopically, petrologically and geochemically. Maceral analyses reveal a dominance of duroclarite to clarodurite subgroups. The synthesis of source rock characteristics emphatically surmises that in the Kalaris member, organic matter is ubiquitously of terrestrial origin.

This member displays poor to good and occasionally very good generative potential. The kerogens are predominantly of type III but sometimes type II-III kerogen has also been identified. Such occurrences envisage predominance of gas prone and occasional oil prone source rocks. Vitrinite reflectance values (mostly 0.6 to 1.2% VRo) indicate that the coals are thermally mature.

The depositional environment is interpreted as a peat swamp with a variable density of herbaceous vegetation situated in an upper delta plain.

Keywords: *Caspian, Iran, Rock-Eval, organic geochemistry, petrography, Shemshak*

1-Introduction

Discoveries in petroleum exploration rely on a good analysis of the petroleum system of the given area. The determination of the potential source rocks, their maturity and kinetic parameters, as well as their

extent is among the tasks accomplished by the rapid screening of the rock samples (cores and/or cuttings or outcrops) with the Rock-Eval apparatus.

Southern regions of the Caspian Basin accommodate several significant hydrocarbon reservoirs; however, the source rocks of these hydrocarbons have been not thoroughly investigated. Since debut of the petroleum explorations in west of the Caspian Basin in 1947, several major oil and gas reserves have been discovered (Lebedev 1991). The middle Pliocene sediments in this basin had been considered as the potential source rocks for hydrocarbon reservoirs in this area (Lebedev 1991). However, they are lean and containing only about 0.3-0.6% wt organic material (OM), and have not reached sufficient maturity for the petroleum generation (Lebedev 1991). So far, the potential source rocks of the area has been evaluated through geochemical in different sectors of the basin (Narimanov 1994, Saint et al. 1997, Belopolsky and Talwani, 1999, Nechayeva and Grayzer 2000).

Thick organic-rich strata of the Shemshak Formation, which ranges from upper Triassic to lower Jurassic is extended over the southern districts of the Caspian Basin, in the Alborz mountain range and in the Central Iran tectonic zone. This unit is OM-rich and accommodates several important coal deposits. The thick organic and coal-rich sediments of the Shemshak Formation were deposited in the fluviodeltaic environment (Zamani et al., 2000).

Southern Caspian Basin is rather exceptional in some aspects such as abnormally low geothermal gradient with rapid heat flow, high sedimentation rates and subsidence (Schoellkopf et al. 1997). Accordingly, the upper boundary of the oil generation window in this area has been encountered in depth range of 6-8km; onset of the wet gas, condensates and light oil generation is at 8 to 13km, and dry gas generation starts at about 10 to 15 km. The considerable thickness of the sediments in the margins of this basin, that include of about 1.5-2km Quaternary sediments; 5-8km upper Miocene-Pliocene, and 8-12km Mesozoic-Paleocene (Berberian 1983), suggests that, despite the low geothermal gradient in the area, the Shemshak Formation has achieved required burial depth for the oil and gas generation.

Geochemical investigations by Narimanov (1994) revealed that in the southern Caspian, sediments up to 9km depth could be important source rocks for hydrocarbon reserves of this area, and hydrocarbon generation is not entirely limited to deep central parts of this basin.

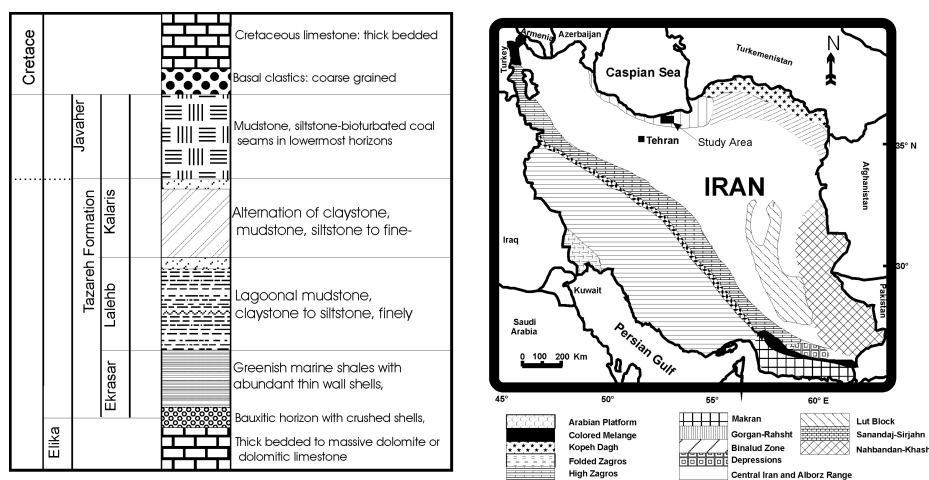
In this paper different techniques including organic and inorganic petrography and Rock-Eval Pyrolysis have been employed to evaluate amount, type and the maturation levels of the kerogens of the Kalaris member from the Shemshak Formation in the Galandrud area. Results of the Rock-Eval analysis have been compared with petrographic data to acquire a better understanding of the source rock characters and maturation.

2- Geological setting

Triassic marine transgression over the Permian sediments caused deposition of the carbonate sediment of the Elika Formation in the northern Iran. Most parts of Iran were uplifted during the early Cimmerian orogeny in the late Triassic. This event caused prevalence of the fluviodeltaic system and development of extensive coal swamp in the late Triassic - lower Jurassic time throughout central Iran and Alborz area. Subsequently, deposition of the transgressive marine carbonates such as Delichi and Lar Formation in the middle Jurassic continued to late Cretaceous. Laramide orogeny in this time shaped main outlines of the Alborz mountain ranges.

In the study area, the Elika Formation of lower to middle Triassic is the oldest unit and composed of nummulitic limestone and dolomite. The Shemshak Formation with a fault contact overlies this unit in the studied area. The Shemshak Formation has been divided into four members in the area, Ekrasar (Ek), Laleband (La), Kalaris (Ka) and Javaherdeh (Ja). These members crop out in the core of an anticline with a WNW-ESE trend. Transgressive marine green shales of the Ek member, of about 100m thickness, overlie Elika Formation. The La member consists of 600m mudstone, claystone, siltstone with well preserved laminations, some bioturbation (swamp facies) and few coal beds in the uppermost of the unit. The Ka member, which is the main subject of this study, composed of 700m sequence of argillites, siltstone, sandstone, coaly shales and coal beds. Remains of the fossil

plants such as *Dictyophyllous*, *Coniopteris*, and palynomorphs such as *Rhaetipollis germanicus schulz* and *Kyrtoisporis specious madler* all are indications of the Rhaetian stage. This member is sandwiched between two sandstone key beds in the lower and uppermost parts. The Ja member consists of 500m siltstone and mudstone with extensive bioturbation and unworkable coal lenses and beds. Its lithology shows close similarity with the La member and is indicative of a shallow clastic sedimentary setting. The Cretaceous Tizkuh Formation conformably overlies the latter unit with basal transgressive conglomerates (Fig. 1).



3- Methods

Two hundred samples were collected from the Galandrud coal mine (tunnel # 6 and wells # 18, 20 and 29). Thin and polished sections were prepared for rock matrix and OM study. To study the petrography, diagenesis and depositional environment of these strata, 120 thin sections from various lithologies were also prepared.

Rock-Eval Pyrolysis analysis was carried out on eighty samples by Oil Show Analyzer using 100mg of pulverized whole rock samples. After initial heating at 300°C in a helium atmosphere, the temperature is then programmed to increase about 25°C/min up to 600°C. The vapor was analyzed with a flame ionization detector and results were shown as pyrograms and tables. A thermal conductivity detector later measured the amount of CO₂ trapped in a chamber throughout the analysis.

Twenty samples out of eighty, which were analyzed by Rock-Eval pyrolysis and showed higher potential for hydrocarbon generation, have been selected for detailed study in transmitted, reflected and ultra violet (UV) lights. Prior to any petrographic examination of the OM, kerogen concentration is an essential step. First, rock samples were cleaned by compressed air, rinsed in the deionized water, then dried and crushed. Next step was demineralization that fulfilled with carbonate removal by hydrochloric acid. Quartz and silicate removal from samples was carried out by hydrofluoric acid treatment. Pyrites were removed from samples using sodium borohydride solution (Padley et al., 1991). Remaining minerals in the samples were dissolved by boron fluoride (BF₃) (Roble and Davis, 1993). Separation of kerogen from remaining minerals was performed by standard procedure (Durand and Nicaise, 1980). Pellets of extracted kerogens have been prepared by mounting them in a hole in a methyl metacrylate chip, and then the hole was filled by epoxy and hardener. Later, the pellets were polished in four steps to get best results in the reflected light petrography. Polished slides of the whole rock samples were also prepared for transmitted light petrography.

4- Organic Petrography

Organic petrology uses reflected light microscopy to characterize dispersed organic matter in rocks, in terms of macerals and organic facies, as well as source rock maturation. Whole samples and extracted

kerogen from different cores and cuttings of the Shemshak Formation were examined in the transmitted, reflected and ultra violet (UV) lights, to determine the levels of maturation and potential of hydrocarbon generation by this unit in the study area.

4-1- Transmitted light microscopy: Different groups of OM have been distinguished in slides, which include:

1- Amorphous OM consists of subcolloidal, granulose, grumeluse that show some fluorescence under the Ultra Violet light (UV). This group of OM is almost transparent and show light brown to dark brown colors (Figs. 2 and 3).

2- Herbaceous OM consists of tissues, cuticles, spores and pollens and shows some fluorescence under the UV light (Figs. 3 and 4).

3- Woody OM includes ligneux fragments and gelifée (Figs. 5 and 6).

4- Coaly OM includes different opaque materials (Fig 6).

Source of the amorphous OM could be planktonic and usually show good potential for hydrocarbon generation (Massoud and Kinghorn 1985). The hydrogen index of samples increases with richness of samples with amorphous OM (Fig. 7). This indicates that this group of OM is hydrogen rich and has good potential for hydrocarbon generation. The Herbaceous OM also shows high hydrogen content (Fig. 7) and even has potential for liquid hydrocarbon generation (Teichmüller 1986). In contrast, hydrogen index decreases with an increase in the amount of woody and coaly OM in the samples (Fig. 7). This observation is an indication of their low potential for liquid hydrocarbon generation.

Using point-counting method, abundance of different OM groups have been estimated. Accordingly, amorphous, woody and coaly OM were the main constituents while herbaceous materials were almost absent (Fig 8).

Thermal Alteration Index (TAI) of spores and pollens in different slides (Fig. 3) ranges from +2 to -3 which is equivalent with high volatile bituminous coals (Bustin et al., 1986).

4-2- Incident light microscopy: Different groups of the macerals have been examined in pellets under incident and UV lights. Relative abundance of the different maceral groups were determined by the

point-counting and MPV GEOP software. Volume percent of each group was calculated using MPV GEOP (Figs. 9 and 10).

One of the most important maceral groups in the studied samples is vitrinite, which includes three subgroups according to Australian maceral classification system. The subgroup of telovitrinite that is formed by vitrinitization of herbal tissues, shows cellular microstructure which are occasionally filled by mineral matters or resinite and other macerals (Fig. 11). Its cellular fabric is well-preserved (δ and δ types) which suggests moderate maturation. The other subgroup of the vitrinite is detrovitrinite, which has been formed from vitrinitization of autochthonous or allochthonous herbal fragments. The oxidation of gelovitrinite along microfractures could be seen in some samples (Fig. 12).

The inertinite maceral group is accordingly subdivided into several groups. The fusinite macerals are banded or amorphous with clear herbal microstructures. While, pyrofusinite forms during bush fires and shows distinct herbal microstructure with light yellow color (Fig. 13), oxyfusinite is product of the fusinite subaerial and biological oxidation and do not show distinct microstructures (Fig. 14). The sclerotinite subgroup shows cellular microstructure with gray to white colors (Fig. 15).

Measured vitrinite reflectance of the concentrated kerogens on the polished pellets show a unimodal pattern (Fig. 16). Mean vitrinite reflectance (VRo%) and tenfold reflectance in the air (10Ra) were also measured in samples from different depths (Table 1).

Table. 1

| SAMPLE NO. | Rom % | DEPTH (m) | 10Ra | LITHOLOGY |
|------------|--------|-----------|------|-------------|
| Z170/R-71 | 7170e | 71 | 71e | Silty shale |
| Z171/R-71 | 7171n | 71n | 71n | Coal |
| Z171+ | 7171+ | 71+ | 71+ | Siltstone |
| Z171 | 7171 | 71 | 71 | Silty shale |
| Z172 | 7172 | 72 | 72 | Claystone |
| Z173S | 7173S | 73S | 73S | Claystone |
| Z172 | 7172 | 72 | 72 | Coal |
| Z172 | 7172 | 72 | 72 | Claystone |
| Z172 | 7172 | 72 | 72 | Coal |
| Z172 | 7172 | 72 | 72 | Siltstone |
| Z172+ | 7172+ | 72+ | 72+ | Shale |
| Z172° | 7172° | 72° | 72° | Siltstone |
| Z17999 | 71799 | 799 | 799 | Siltstone |
| Z172° | 7172° | 72° | 72° | Claystone |
| Z170C | 7170C | 70C | 70C | Claystone |
| Z171P1 | 7171P1 | 71P1 | 71P1 | Silty shale |
| Z170P0 | 7170P0 | 70P0 | 70P0 | Shale |
| Z172x | 7172x | 72x | 72x | Siltstone |
| Z172 | 7172 | 72 | 72 | Claystone |
| Z170e | 7170e | 70e | 70e | Shale |

Table.1. VRo%, depth, 10Ra and lithology for different samples.

4-3- Fluorescence microscopy: Spectral fluorescence photometry had been used to determine maturation level of OM. Alterations in the fluorescence intensity and color was measured after 30 minutes excitation of each sample. Samples with lower levels of maturity showed positive alterations while more mature ones displayed negative alterations. Sporinite showed yellow to greenish yellow fluorescence that is indicative of a maturation level corresponding to the upper threshold of the oil generation window. These observations are indicative of the maturity level equivalent to about 0.6 to 0.9% VRo, which is in accordance with the vitrinite reflectance measurements.

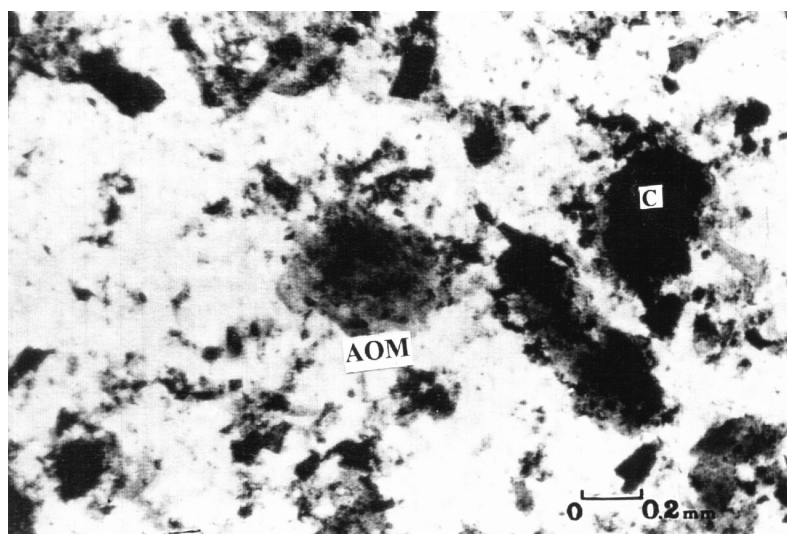


Figure 2 - Amorphous OM of subcolloidal grumeluse (AOM) type along with some coal particles (C) (Transmitted normal light).

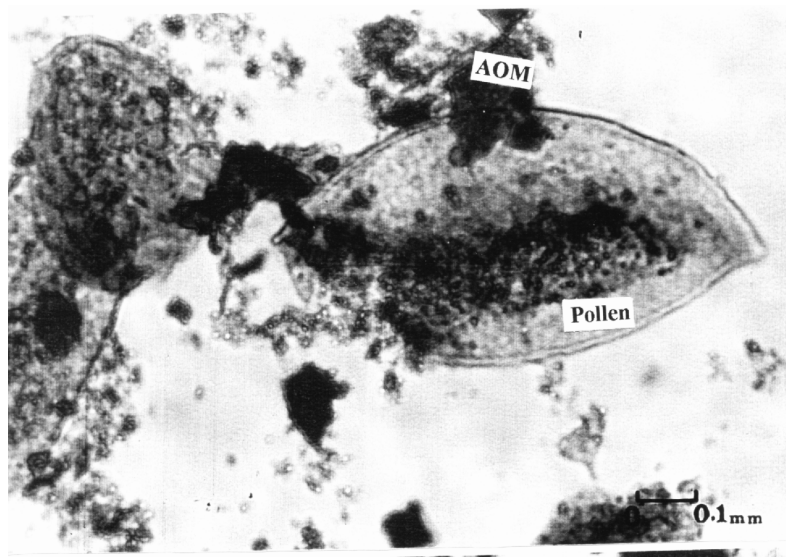


Figure 3 - Pollens along with some grumeluse amorphous OM (Transmitted normal light).

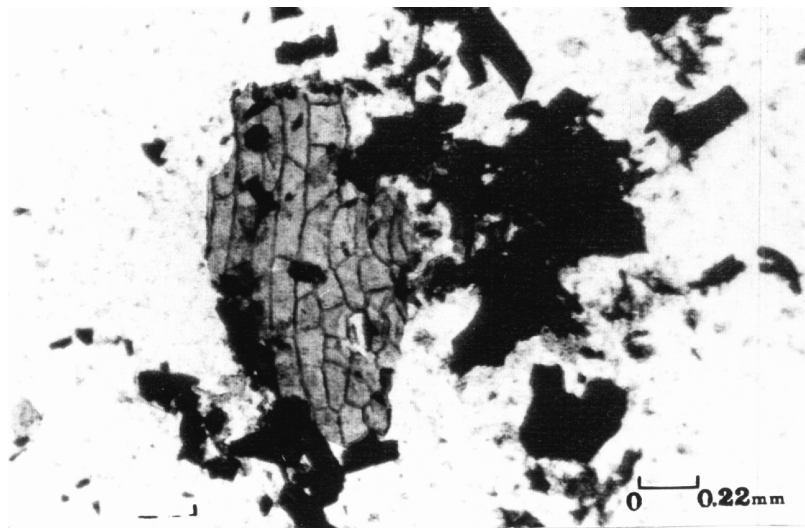


Figure 4 - A large cuticle particle with its characteristic cellular structure along with some coal particles (Transmitted normal light).

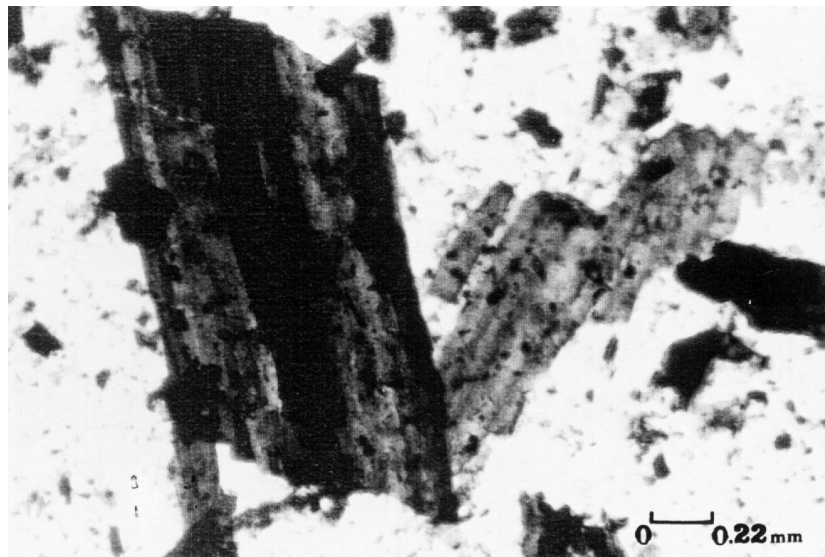


Figure 5 - Large particles of the woody ligneous fragments (Transmitted normal light).

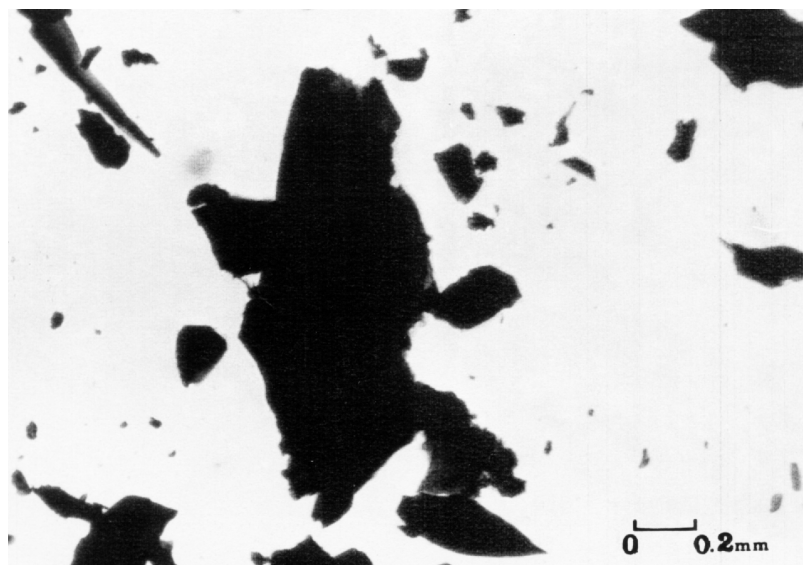


Figure 6 - Large particles of the gelified OM with brown margins (Transmitted normal light).

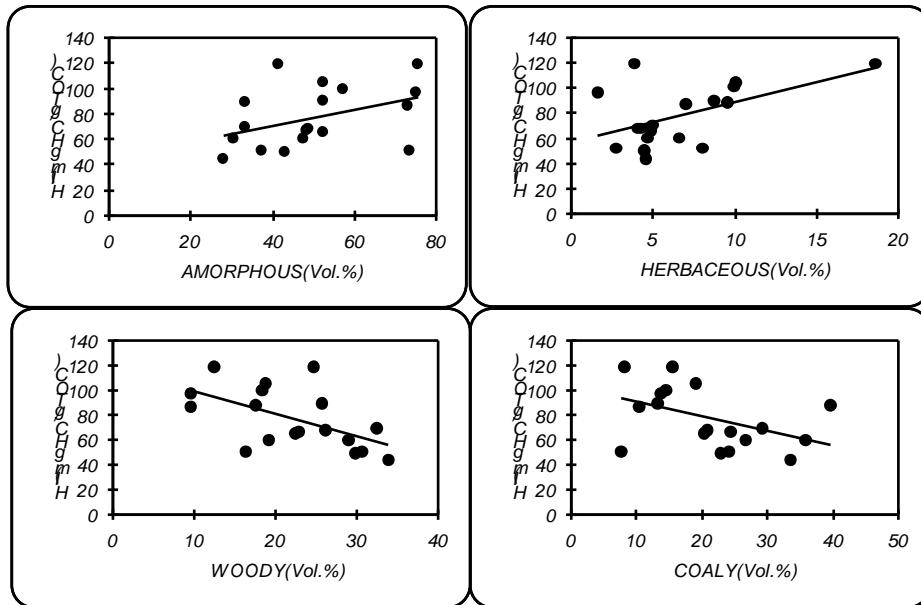


Figure 7 - The HI variations in different OM groups.

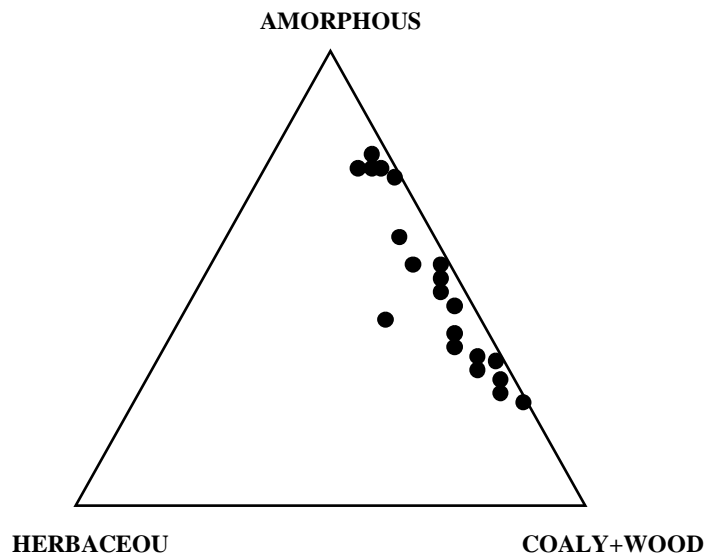


Figure 8 - The ternary diagram of different OM measured under transmitted light.

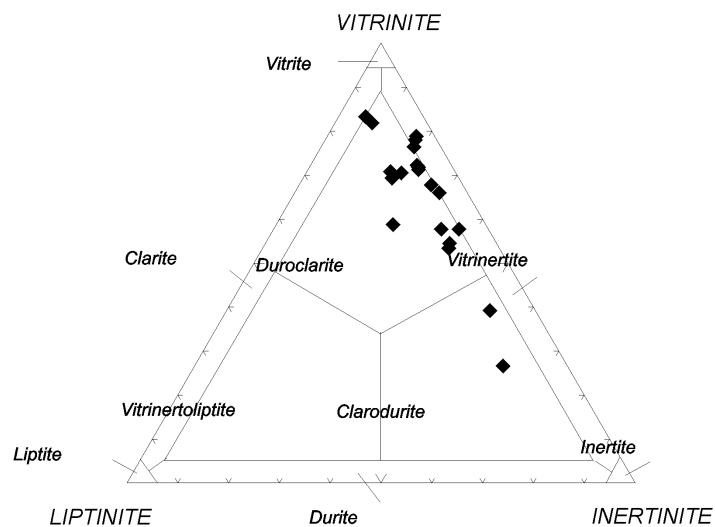


Figure 9 - The ternary diagram of different microlithotypes in the studied samples.

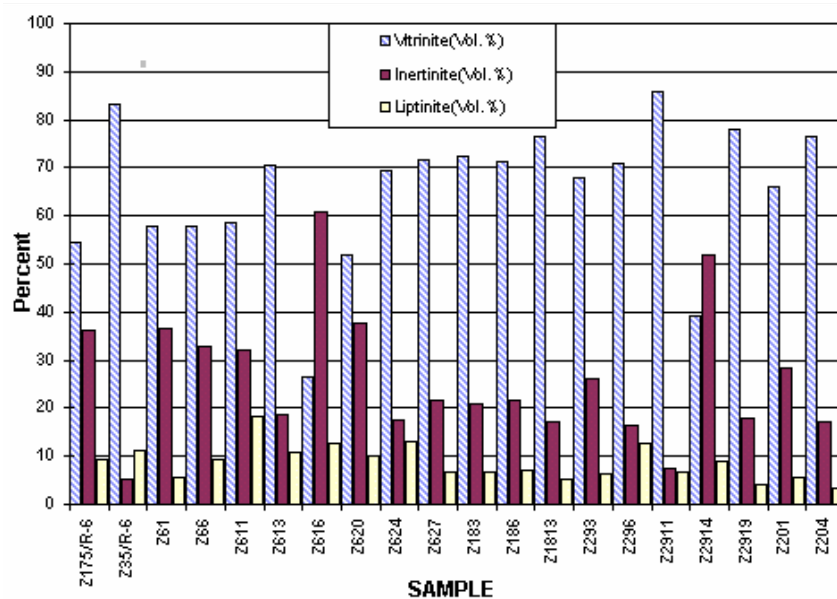


Figure 10 - Histogram of the point counting data for main maceral groups in the incident and UV lights.

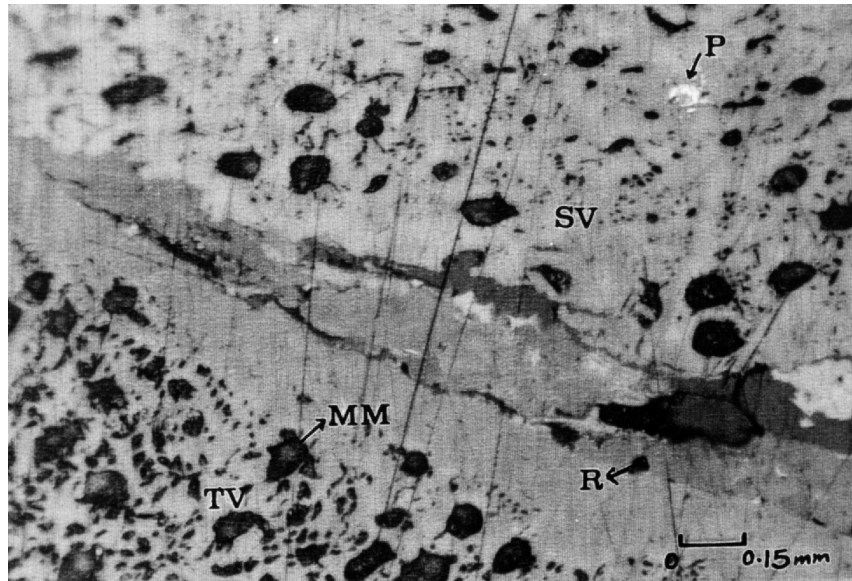


Figure 11 - The telovitrinite (TV) with fillings of mineral material (MM), resinite (R), semivitrinite (SV) and pyrite (P) (Incident light).

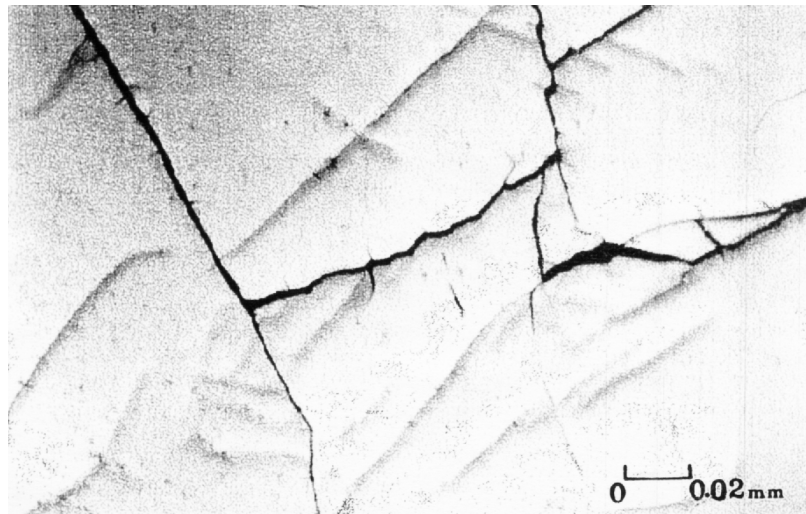


Figure 12 - Oxidation of gelocollinite maceral along fractures (Incident light).

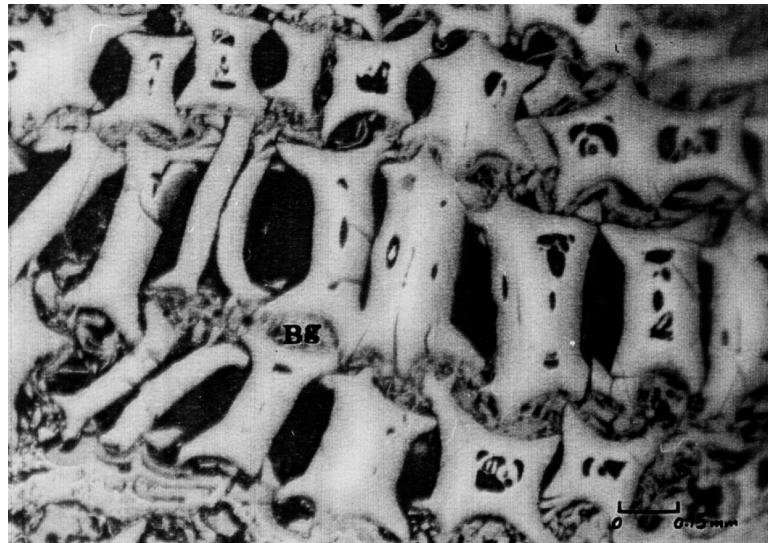


Figure 13 - Pyrofusinite with its characteristic cellular structure. In some places (center) Bogen (Bg) structure could also be seen (Incident light).



Figure 14 - A large fragment of oxyfusinite (OF) with fillings of resinite (R) along with particles of other macerals such as vitrinite (V) and mineral matters (Incident light).

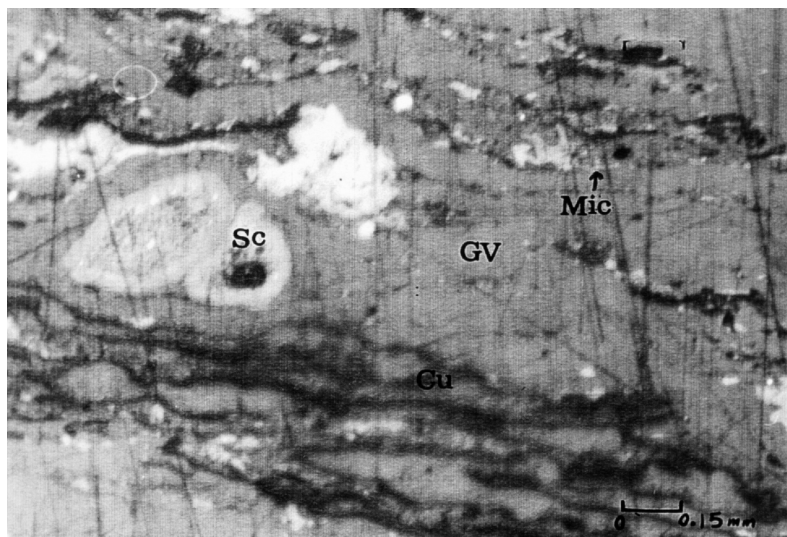


Figure 15 - Micrinite along with macerals of liptinite group such as macrinite (Ma), sclerotinite (Sc), cutinite (Cu) and gelovitrinite (GV) (Incident light).

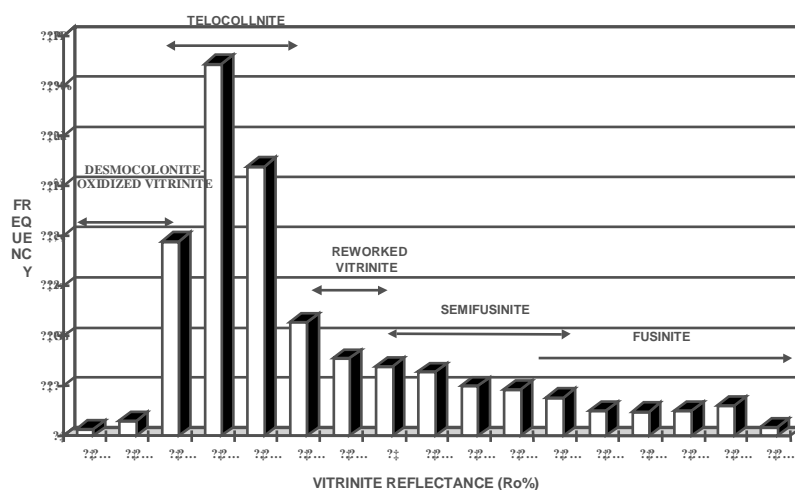


Figure 16 - Histogram of vitrinite reflectance of various maceral groups in the studied samples.

5- Results of Rock-Eval Pyrolysis

In this study Rock-Eval pyrolysis was employed to measure the quantity, quality, and thermal maturity of the OM in the rock samples. Pyrolysis data were supplemented by vitrinite reflectance and spore color (TAI) data to construct geochemical logs. Results of the Rock-Eval pyrolysis are presented in tables 2 and 3. Rock samples with Residual Carbon + Pyrolysed Carbon (RC+PC) values less than 0.5, are considered as lean source rocks with low potential for hydrocarbon generation. Generally, these lean source rocks contain more oxidized OM, while in the high TOC-bearing rocks the OM is mainly lipid-rich and well-preserved (Jones 1987). Type of the OM is also an important controlling factor in hydrocarbon generation. Because the Rock-Eval Pyrolyzer III has been used in this study, HI-Tmax diagrams were employed to distinguish different kerogen types (Figs. 17 and 18). The kerogen identification could be carried out by S₂-TOC diagram (Fig.19) where VRo ranges from 0.5 to 1.0% (Langford et al., 1990). High potential source rocks have minimum S₂ values of about 5 to 10 mgHC/gRock (Table 3, Fig 19). The S₂/ S₃ ratios and HI values exhibit the type of the generated hydrocarbon. The thermal maturation levels were determined by HI-Tmax diagrams (Figs. 17 and 18), which are indicative of early to middle stage of catagenesis. For appraisal of the thermal maturation achieved by different kerogens, the corresponding production index (PI) and the Tmax values have been recommended by several authors (e.g., Peters 1986, Bordenave 1993, Peters and Cassa, 1994). Accordingly, the majority of the studied samples represent the oil generation window. Their average thermal alteration index is estimated to be between 2.6-3.2 and vitrinite reflectance of 0.6 to 1.2% (Figs. 17 and 18, Table.3).

In deltaic sediments with low OM content, which can produce considerable amount of condensate and gas, mineral-matrix effect is high (Hunt 1996). Due to low liquid hydrocarbon generation by kerogen III during pyrolysis, the mineral-matrix effects are enhanced (Espitalie et al., 1984). The regression lines of the TOC pass through

abscissa, which attest mineral-matrix effects and surficial adsorption (Fig.19). The relationship of the different Rock-Eval parameters and constructed geochemical logs are also presented (Figs.20 to 23).

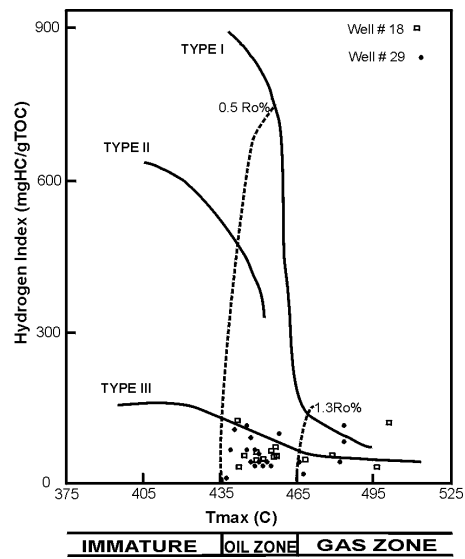


Figure 17 - The HI-Tmax diagram (Hunt 1996) for samples from wells # 18 and 29. Most samples are representing early catagenesis and kerogen III.

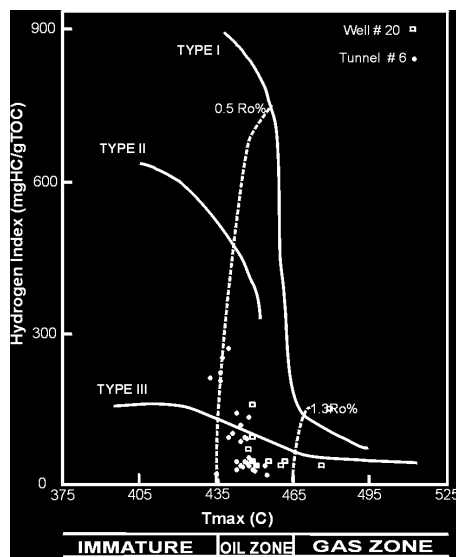


Figure 18 - The HI-Tmax diagram (Hunt 1996) for samples from well # 20 and tunnel # 6. Most samples are representing catagenesis and kerogen type III and some III-II.

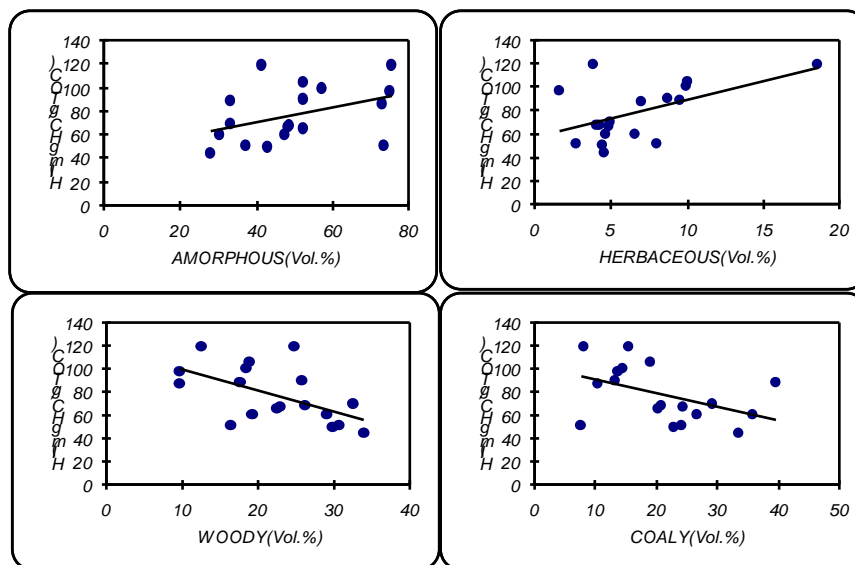


Figure 19 - The S₂-TOC diagram for samples from different wells and tunnel # 6. As shown, most samples present low potential for hydrocarbon generation and representing kerogen III. However, some samples from tunnel # 6 show higher potential for hydrocarbon generation and are kerogen type III-II.

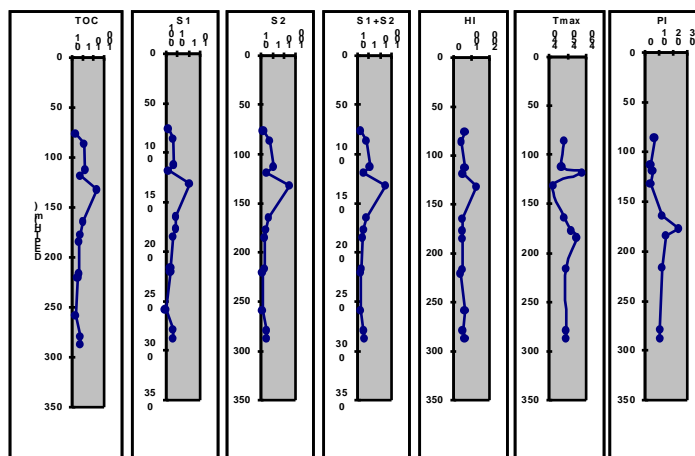


Figure 20 - Geochemical logs for various Rock-Eval parameters versus burial depth for well # 18.

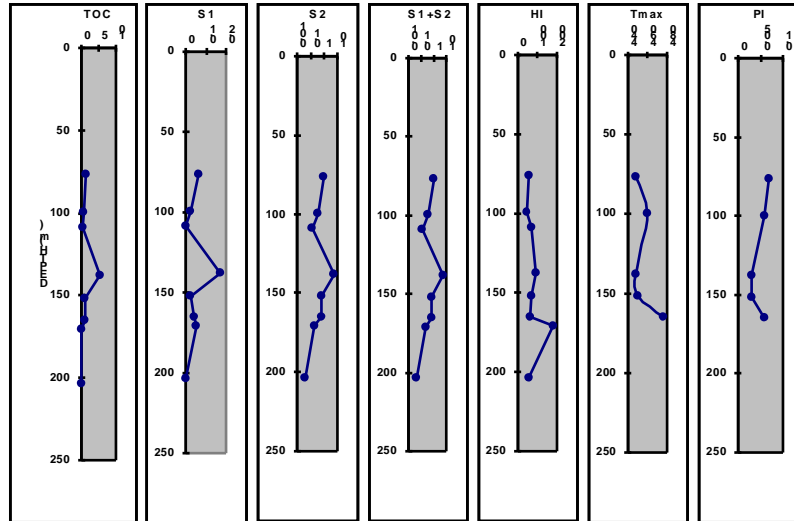


Figure21 - Geochemical logs for various Rock-Eval parameters versus burial depth for well # 20.

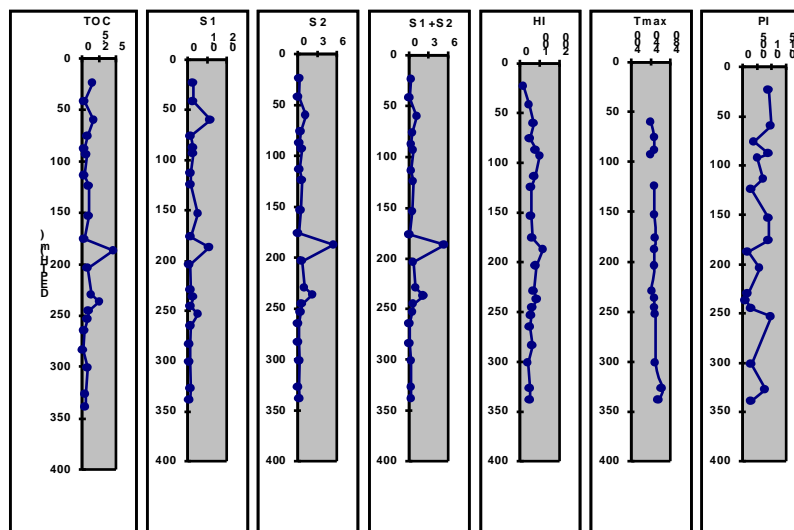


Figure22 - Geochemical logs for various Rock-Eval parameters versus burial depth for tunnel # 6.

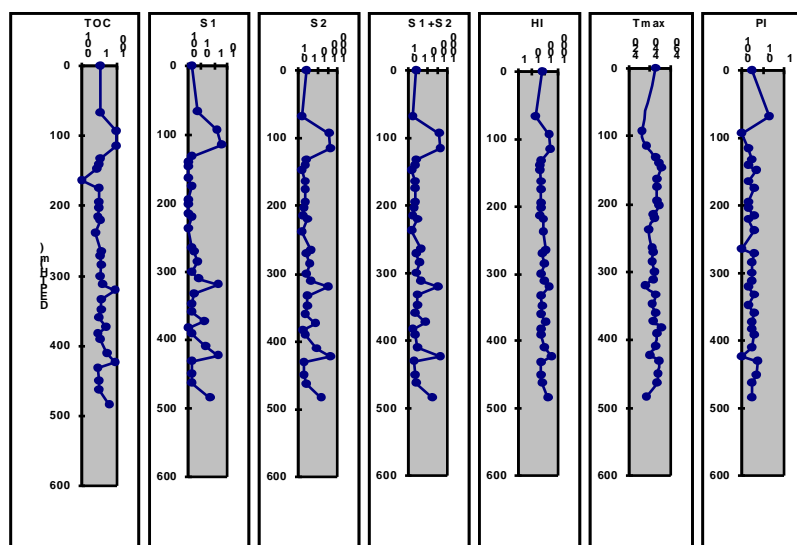


Figure 23 - Geochemical logs for various Rock-Eval parameters versus burial depth for well # 29.

6- Sedimentary Environment

Rad (1986) had proposed a fulviodeltaic system for Shemshak Formation in the eastern Alborz basin. Sedimentologic studies in the Ka member exhibits various features of the fulviodeltaic facies, including fine to medium grained litharnites and siltstone with ripple marks and flasere beddings; mudstone and coal; remains of the different terrestrial plants; horizons of plant's roots; siderite nodules; evaporitic sediments; sabkha dolomites; and lack of marine fossils (Rad 1986). The lower sandstone unit shows features of an abandoned distributary channel fill deposit with graded bedding and ripple marks. Alternations of the natural levees, interdistributary bay, crevasse splay, and swamp deposits have been observed in the main parts of the Ka member. The latter have been sandwiched between two keybed sandstone units. The combination of the lateral channel migrations, the delta movements and the sea-level changes had caused frequent

repetitions in these deposits. During drier seasons in some parts of the delta plain evaporites and sabkha dolomites had been formed. In this climatic conditions, due to sea-level fall in the swamp, formation of inertinite-rich coal had been increased (e.g., McCabe 1984). Lower abundance of the coarse sand compared to the fine-grained mud in this unit suggests a constructive river-dominated deltaic regime. The major coal microlithotypes are duroclarite with some clarodurite as well as more than 50% vitrinite. This implies an upper delta plain system. Besides, low sulfur content of the coals and other sediments and the lack of marine fossils corroborate to this conclusion.

7- Discussion

Because cores and cuttings were not confined after collection all samples show zero S_0 values. In well # 29, S_1 values are less than one and S_2 values are mainly lower than five. The Tmax values of four samples indicate oil window maturity (Table 3) while other samples show low PI values which is due to the low S_1/S_2 ratios. High TOC values in most samples ($>0.5\%$ wt) and $HI < 150$, are indicative of gas generation. Generally, the Tmax values show an increasing trend with burial depth of source rock (Fig. 22). However, some samples, such as sample # 2913, show some discrepancies. The unexpected decrease in the Tmax value of this sample can be attributed to the type of the clay mineral or its OM content. The TOC values show positive correlation with S_1 , S_2 and $S_1 + S_2$, implying mineral-matrix effects. The TOC- S_2 and HI-Tmax diagrams for great number of samples exhibit kerogen type III with level of maturity that corresponds with the early stage of catagenesis (Figs. 19). This level of organic maturation, inferred from Rock-Eval parameters, is compatible with the petrographic examinations and measurements of the vitrinite reflectance (Figs. 17 and 19).

Samples from well # 18 (Table 3) are mainly coal and coaly shales with $S_2 < 5$, which exhibit low mineral-matrix effects and Tmax values. Despite general high HI values, samples of this well have not reached oil generation threshold. The Tmax values in the majority of samples (except No. 181, 1810, and 1811 which show strong mineral-matrix effects) indicate that they are in the early stage of catagenesis. These

values show a general increase with burial depth (Fig. 20). The S_2 -TOC and HI-Tmax diagrams are indicative of the kerogen type III, originated from terrestrial plants (Figs. 17 and 19).

The Tmax values for samples from well # 20 show a general increasing trend with the burial depth and delineating the oil generation window (Figs. 21 and 22, Table 3). The S_2 -TOC and HI-Tmax diagrams designate the kerogen type III that corresponds with oil generation window (Figs. 18 and 19).

Most samples from tunnel # 6 show $S_1 < 1$, but coaly samples exhibit considerable pyrolysis parameters (S_1 , S_2 , $S_1 + S_2$ and TOC) marking generation of the gaseous hydrocarbons along with some oil. Higher values reflected by pyrolysis parameters observed in these samples, comparing with others, are due to the higher TOC values and types of the OM content. These had induced a reduction in the mineral-matrix effects and more realistic Tmax values. The Tmax values show an increasing trend with burial (Fig. 23). Sample No. 100/R-6 shows very high anomalous Tmax values, which could be due to overheating and over-maturation caused by an igneous intrusion that is present in this sampling site. Generally, the pyrolysis parameters show an increasing trend with the TOC content. The S_2 -TOC and HI-Tmax diagrams for most samples are indicative of the kerogen type III, while coaly samples show some contributions from kerogen III-II, as well. This has been inferred from high values of some Rock-Eval parameters such as S_2 and HI. Approximately, majority of the samples shows levels of maturity that corresponds to the early to middle stage of catagenesis (Figs. 18 and 19).

In general, most studied samples, except coals and high TOC samples, show low potential for liquid hydrocarbon generation. Their HI values are less than 150, which make them a gas generative hydrocarbon source rock. Compared with the other samples, coaly and high TOC bearing specimens show high S_1 , S_2 and HI values. This is due to high illite content in most samples, which adsorbs much of the generated liquid hydrocarbons. The other reason is the difference in the type of OM in low and high TOC samples. The latter contains kerogen types III and II-III, while the former are composed mainly of type III.

In general, Rock-Eval data suggest that where this unit attained sufficient levels of maturity it exhibit poor to good potential for the hydrocarbon generation. The vitrinite reflectance, TAI, HI and Tmax values of most samples reveal that the main generated hydrocarbons were generally thermal gas and some waxy and naphthenic oils.

Adopting classification proposed by Jones (1987) for the organic facies and considering the overall hydrogen indices (HI) and the main maceral groups in the studied strata, corresponding organic facies of C and CD could be envisaged for the studied units. Abundance of the terrestrial OM, colinite and telinite macerals and presence of the reworked vitrinite, spores, cuticles, resins, inertinite, and the absence of the algal OM, all are indicative of the fluviodeltaic environments, C and CD organic facies.

8- Conclusion

Evidence from the sedimentology and petrography of the samples indicate a deltaic environment. These include deposits of the abandoned distributary channels, crevasse splay, natural levees, interdistributary bays and swamps. The repetitive nature of these successions was due to the lateral channel, delta movement and sea-level fluctuations. The organic facies are also indicative of the deltaic environment. Taken altogether, it could be suggested that the Ka member represent the uppermost parts of a prograding delta succession.

Rock-Eval Pyrolysis showed that 77% of samples contain more than 0.5% wt OM. The main kerogen type is III and some II-III, which both show gas generation potential but the latter could be oil-prone (heavy oil), as well. Maturation indices such as Tmax, VRo, and liptinite fluorescence are indicative of the lower parts of the oil generation window which is equal to the high volatile bituminous coal (type B, C to A).

Regarding the main kerogen types contained by this unit (i.e. III and II-III), and HI values, it could be concluded that the main generated hydrocarbon was thermal gas. Accordingly, considering the low activation energy of the kerogen III and its level of thermal maturation for the studied samples, generation of major amounts of gas could be

expected. The presence of some resinite with this level of thermal maturation suggests generation of some waxy oils, light naphthenic oils and some naphthenic condensates, as well.

In the southern Caspian Basin most hydrocarbon reservoirs are hosted by Chelkan Formation of the middle Pliocene. Regarding substantiated upward hydrocarbon migration to the Chelkan Formation and the lack of potential for hydrocarbon generation by this unit, the source of the reservoired hydrocarbon should be sought in the OM-rich underlying units, such as Shemshak Formation. The Mesozoic active growth faults, characteristic of the deltaic environments, by generating well-developed microfracture systems in the source rock, had facilitated upward petroleum migration.

Acknowledgements:

The authors are grateful to Iranian National Oil Company, Research Institute of Petroleum Industry for providing facilities and financing the project. The Tehran University is also acknowledged for providing a research grant (No.512.1.386) to the first author.

References:

- Belopol'sky, A.V., Talwani, M., (1999) *Petroleum reserves and potential of the greater Caspian region*. American Association of Petroleum Geologists International Conference and Exhibition; abstracts. American Association of Petroleum Geologists Bulletin. 83, 8.
- Berberian, M., (1983) *The southern Caspian: A Compressional depression floored by a trapped modified ocean crust*, Canadian Journal of Earth Sciences **20**, 163- 183.
- Bordenave, M.L., (1993) *Applied petroleum geochemistry*, Paris, Editions Technip.
- Bustin, R.M., Cameron, A.R., Grieve, D.A., W.D. Kalkreuth, (1989) *Coal petrology, it's principles, methods, and applications*, Geological Association of Canada, Short Course Notes 3.
- Durand, B., G. Nicaise, (1980) *Procedures for kerogen isolation*. In Durand, B. (Ed.) *Kerogen*, Paris, Editions Technip 35-53.

- Espitalie, J., Makadi, K.S. J., Trichet, (1984) *Role of the mineral matrix during kerogen pyrolysis*, Organic Geochemistry **6**, 365-382.
- Hunt, J.W., (1996) *Petroleum geochemistry and geology*, 2nd ed., New York, W. H. Freeman and Company.
- Jones, R.W., (1987) *Organic facies*. In Brooks, J. and Welte, D. (Eds.) *Advances in petroleum geochemistry*, London, Academic Press 2 , pp.1-90.
- Langford, F.F., Blance, M.M.V., (1990) *Interpreting rock-Eval pyrolysis data using graphs of pyrolyzable hydrocarbons vs. total organic carbon*, American Association of Petroleum Geologists Bulletin, **74**, 799-804.
- Lebedev, J., (1991) *Oil and gas potential of the Caspian Sea*, petroleum information cooperation.
- McCabe, P.J., (1984) *Depositional environments of coal and coal bearing strata*, Spec. Publs. IAS Sp. Pub. **7**, 13-42.
- Narimanov, A.A., (1994) *The South Caspian oil and gas basin reservoirs, formation and their oil and gas saturation*. Annual Meeting Abstracts - American Association of Petroleum Geologists and Society of Economic Paleontologists and Mineralogists. 125-127.
- Nechayeva, O.L., Grayzer, E.M., (2000) *Characteristics of oils and condensates of sub-salt sediments of North Caspian oil-gas province*. Petroleum Geology, a Quarterly Journal **34**, 288-293.
- Padley, D., Michaelsen, B.H., McKirdy, D., (1991) *Organic geochemical procedures, A protocol of preparative geochemistry*, Organic geochemistry laboratory, Department of geology and geophysics, the university of Adelaide, Australia, **2**, 21-24.
- Peters, K.E., (1986) *Guidelines for evaluating petroleum source rock using programmed pyrolysis*, American Association of Petroleum Geologists Bulletin, **70**, 318-329.
- Peters, K.E., Cassa, M.R., (1994) *Applied source rock geochemistry*. In Magoon L. B., and Dow, W.G.(Eds.)*The petroleum system from source to trap*, Tulsa, American Association of Petroleum Geologists Memoir 60.
- Petersen, H.I., Andsbjerg, J., Bojesen, J.A., Nytoft, H.P., (2000) *Organic facies and petroleum potential of the Oligocene-lower*

-
- Miocene sources rocks from Crimea to Azarbaijan*. Journal of Petroleum Geology **23**, 55-90.
- Rad, F.R., (1986) *A Jurassic delta in the eastern Alborz, NE Iran*, Journal of Petroleum Geology **9**, 281-294.
- Roble, T.L., Davis, B.H., (1993) *Comparison of the HF-HCl and HF-BF₃ maceration techniques and the chemistry of result organic concentrates*, Organic Geochemistry **20**, 249-255.
- Saint, G.M., Baudin, F., Bazhenova, O.K., Fadeeva. N., (1997) *Organic facies and petroleum potential of the Oligocene-lower Miocene sources rocks from Crimea to Azerbaijan*. American Association of Petroleum Geologists International Conference and Exhibition; abstracts, American Association of Petroleum Geologists Bulletin 81, 8.
- Schoellkopf, N., Jeremy, B., Dahl, E., B.J. Murphy, (1997) *Geochemical maturation modelling and petroleum systems, offshore Azarbaijan, South Caspian Sea, abstract*, American Association of Petroleum Geologists Bulletin, 81, 1410.
- Smyth, M., (1984) *Coal microlithotype related to sedimentary environments in the Cooper basin, Australia*, Spec. Pub. Int. Ass. Sed., **7**, 333-347.
- Snowdon, L.R., (1991) *Oil from type III organic matter, resinite revisited*, Organic Geochemistry, **17**, 743-747.
- Zamani, Z, Kamali, M.R. and Rahimpour-Bonab, H., (2000) *Source-rock evaluation and geochemical measurement of thermal maturity in upper Triassic and lower Jurassic sediments*, Central Alborz, Iran. GeoArabia, Middle east Petroleum Sciences, **5**, 200-201.

